

Systematic study on production of hidden-bottom pentaquark via γp and $\pi^- p$ scatterings

Xiao-Yun Wang,^{1,*} Jun He,^{2,†} and Xurong Chen^{3,4,5,‡}

¹*Department of physics, Lanzhou University of Technology, Lanzhou 730050, China*

²*Department of Physics and Institute of Theoretical Physics,
Nanjing Normal University, Nanjing, Jiangsu 210097, China*

³*Institute of Modern Physics, Chinese Academy of Sciences, Lanzhou 730000, China*

⁴*University of Chinese Academy of Sciences, Beijing 100049*

⁵*Institute of Quantum Matter, South China Normal University, Guangzhou 510006, China*

In this work, the production of hidden-bottom pentaquark P_b states via γp and $\pi^- p$ scatterings is studied within an effective Lagrangian approach and the vector-meson-dominance mechanism. For the P_b production in the process $\gamma p \rightarrow \Upsilon p$, the dipole Pomeron model is employed to calculate the background contribution, and the experimental data can be well described. For the process $\pi^- p \rightarrow \Upsilon n$, the Reggeized t -channel with π exchange is considered as the main background for the P_b production. The cross section from t -channel π exchange is very small due to weak coupling of P_b state to the $\pi\pi$ channel predicted theoretically. Near the threshold, two-peak structure from the states $P_b(11080)$ and $P_b(11125)$ can be observed if energy bin width is chosen as 0.01 GeV, and the same result is obtained in the $\pi^- p$ scattering. Moreover, by taking the branching ratio of $\text{Br}[P_b \rightarrow \pi N] \simeq 0.05\%$, the numerical result shows that the average value of cross section from the $P_b(11080)$ state produced in the γp or $\pi^- p$ scattering reaches at least 0.1 nb with a bin of 0.1 GeV. Even if we reduce the branching ratio of the P_b state into πN channel by one order, the theoretical average of the cross section from $P_b(11080)$ production in $\pi^- p$ scattering can reach the order of 0.01 nb with a bin of 0.1 GeV, which means that the signal can still be clearly distinguished from the background. The experimental measurements and studies on the hidden-bottom pentaquark P_b state production in the γp or $\pi^- p$ scattering near-threshold energy region around $W \simeq 11$ GeV are strongly suggested, which are accessible at COMPASS and JPARC. Particularly, the result of the photoproduction suggests that it is very promising to observe the hidden-bottom pentaquark at proposed EicC facility in China.

PACS numbers: 13.60.Rj, 11.10.Ef, 12.40.Vv, 12.40.Nn

I. INTRODUCTION

Recently, three narrow hidden-charm pentaquark states, $P_c(4312)$, $P_c(4440)$ and $P_c(4457)$, were observed by the LHCb Collaboration [1]. It is interesting that $P_c(4440)$ and $P_c(4457)$ are two peaks, which are revolved from the previously discovered $P_c(4450)$ [2]. Moreover, it is found that these three P_c states are quite narrow, and can be clearly seen in the $J/\psi p$ invariant mass spectrum [1]. As it was mentioned in Ref. [1] that these three P_c states are very good candidates of molecular states, but the explanations of them as tightly bound pentaquarks cannot be ruled out. Soon after these P_c states were discovered, the attempts to understand their internal structure were performed in a large amount of theoretical models [3–19]. However, more experimental and theoretical research is still needed to justify which one of these explanations is the real origin of these exotic states. Moreover, as shown in the Review of Particle Physics (PDG) [20], although many exotic hadrons were listed, most of them were observed in the electron-positron or proton-proton collision. Hence, production of these exotic hadrons in more different mechanisms is very important to understand their nature.

Up to now, the hidden-charm pentaquarks were only observed in the Λ_b decay at LHCb. Production of the pentaquarks in other ways is very helpful to obtain the definite

evidence for the P_c states as genuine states. Different methods were proposed to detect the newly observed P_c states including photoproduction [21, 22] and $\pi^- p$ scattering [23]. Recently, the measurement of the process $\gamma p \rightarrow J/\psi p$ was reported by the GlueX Collaboration [24]. Although the signal of the P_c state was not detected due to insufficient experimental precision, the branching ratio of the P_c state decaying to $J/\psi p$ given by the experiment is consistent with our previous theoretical prediction [22].

The hidden-charm pentaquark is a quark system composed of three light quarks and a charm quark pair. It is natural to extend it to the bottom sector to predict hidden-bottom pentaquark which contains a bottom quark pair. Such extension is more reasonable in the molecular state picture which is widely adopted to explain the P_c states [3–5, 7, 11, 12, 16, 25, 26]. Due to the existence of the heavy quark symmetry, the $\Sigma_b^{(*)} B$ interaction is analogous to the $\Sigma_c^{(*)} \bar{D}$ interaction, which will lead to the existence of hidden-bottom pentaquark. Such similarity has been found in the comparison between the states $Z_b(10610)$ and $Z_b(10650)$ in bottom sector and the states $Z_c(3900)$ and $Z_c(4020)$ in charm sector. Based on such justification, many predictions about the hidden-bottom pentaquarks have been given within different theoretical models [27–35].

It is interesting to study the possibility to observe such hidden-bottom pentaquark in future experiment. The P_c states were observed in the Λ_b decay at LHCb. However, it is impossible to find an analogous decay for hidden-bottom pentaquark. If we recall that such pentaquarks are composed of three light quarks and a heavy quark pair, it is reasonable to

* xywang01@outlook.com

† Corresponding author: junhe@nynu.edu.cn

‡ xchen@impcas.ac.cn

produce them by exciting the nucleon by photon or pion meson to drag out a hidden-bottom quark pair. Hence, in the current work, we will study the possibility of production of hidden bottom pentaquark P_b states via γp and $\pi^- p$ scatterings.

Because such states are still not observed in experiment, we need the theoretical decay width to make the prediction. One notices that in a recent paper [35], the authors predicted a series of hidden-bottom pentaquark states based on the observed three P_c states within the hadron molecular state model, and the decay widths of these states into the Υp channel were also provided in their work. The mass and decay properties of the $P_b(11080)$ state predicted in Ref. [35] are also consistent with the prediction about a $N^*(11100)$ state in Ref. [27].

In the current work, the production of the hidden-bottom pentaquark P_b states via reactions $\gamma p \rightarrow \Upsilon p$ and $\pi^- p \rightarrow \Upsilon n$ will be investigated within the framework of an effective Lagrangian approach and the vector-meson-dominance (VMD) model. The basic Feynman diagrams of the reaction $\gamma p \rightarrow \Upsilon p$ are illustrated in Fig. 1 where the pentaquarks P_b are produced through s - and u -channels. Fig. 1(c) depicts the Pomeron exchange process, which is considered as the mainly background contribution. Considering the off-shell effect of the intermediate P_b states, the u -channel contribution in γp or $\pi^- p$ scattering will be neglected in our calculation.

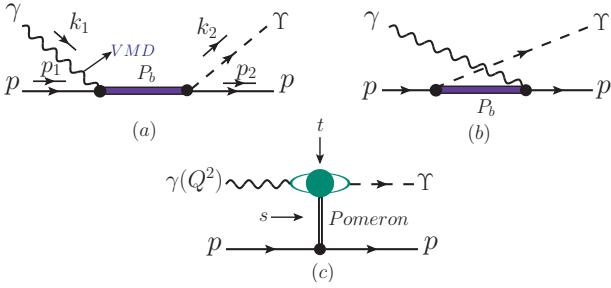


FIG. 1. Feynman diagrams for the reaction $\gamma p \rightarrow \Upsilon p$.

In Fig. 2(a)-(b), the Feynman diagrams are presented for describing the P_b production in the reaction $\pi^- p \rightarrow \Upsilon n$ at tree level. Moreover, the Reggeized t channel will be responsible for describing the main background, as depicted in Fig. 2(c).

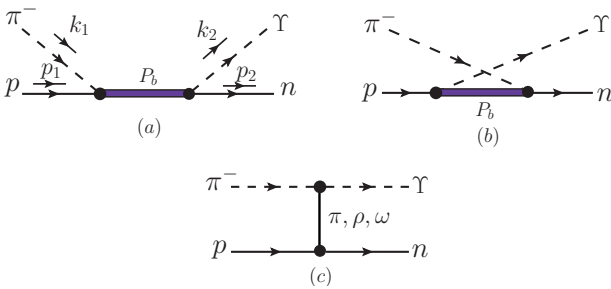


FIG. 2. Feynman diagrams for the reaction $\pi^- p \rightarrow \Upsilon n$.

This paper is organized as follows. After the introduction,

we present the formalism including Lagrangians and amplitudes for the reactions $\gamma p \rightarrow \Upsilon p$ and $\pi^- p \rightarrow \Upsilon n$ in Section II. The numerical results of the cross section follow in Section III. Finally, the paper ends with a brief summary.

II. FORMALISM

A. Lagrangians for the P_b production

Since the P_b states have not been found experimentally, in this work, the spin-parity quantum number of the P_b state is taken as $J^P = 1/2^-$ as suggested in Refs. [27, 35]. For describing the P_b production in photon and pion induced processes, the following Lagrangians are needed [22, 23, 36–38],

$$\mathcal{L}_{\gamma NP_b} = \frac{eh}{2m_N} \bar{N} \sigma_{\mu\nu} \partial^\nu A^\mu P_b + \text{H.c.}, \quad (1)$$

$$\mathcal{L}_{P_b \Upsilon N} = g_{P_b \Upsilon N} \bar{N} \gamma_5 \gamma_\mu P_b \Upsilon^\mu + \text{H.c.}, \quad (2)$$

$$\mathcal{L}_{\pi NP_b} = g_{\pi NP_b} \bar{N} \vec{\tau} \cdot \vec{\pi} P_b + \text{H.c.}, \quad (3)$$

where N , A , P_b , π and Υ are the nucleon, photon, P_b state, pion, and Υ meson fields, respectively. And τ is the Pauli matrix.

The values of coupling constants $g_{P_b \Upsilon N}$ and $g_{\pi NP_b}$ can be derived from the corresponding decay width

$$\Gamma_{P_b \rightarrow \Upsilon N} = \frac{|\vec{p}_\Upsilon^{\text{c.m.}}|}{16\pi m_{P_b}^2} |\mathcal{M}_{P_b \rightarrow \Upsilon N}|^2, \quad (4)$$

$$\Gamma_{P_b \rightarrow \pi N} = \frac{3g_{\pi NP_b}^2 (m_N + E_N)}{4\pi m_{P_b}} |\vec{p}_N^{\text{c.m.}}|, \quad (5)$$

with

$$|\vec{p}_\Upsilon^{\text{c.m.}}| = \frac{\lambda(m_{P_b}^2, m_\Upsilon^2, m_N^2)}{2m_{P_b}}, \quad (6)$$

$$|\vec{p}_N^{\text{c.m.}}| = \frac{\lambda(m_{P_b}^2, m_\pi^2, m_N^2)}{2m_{P_b}}, \quad (7)$$

$$E_N = \sqrt{|\vec{p}_N^{\text{c.m.}}|^2 + m_N^2}, \quad (8)$$

where λ is the Källén function with $\lambda(x, y, z) \equiv \sqrt{(x - y - z)^2 - 4yz}$, and $\mathcal{M}_{P_b \rightarrow \Upsilon N}$ is the decay amplitudes. The m_{P_b} , m_Υ , m_N , and m_π are the masses of P_b , Υ , nucleon, and pion meson, respectively.

For the electromagnetic (EM) coupling eh related to the γNP_b vertex, its value can be obtained from the strong coupling constant $g_{P_b \Upsilon N}$ within the VMD mechanism [39–41]. The EM coupling constants eh are related to the coupling constants $g_{P_b \Upsilon N}$ as

$$eh = g_{P_b \Upsilon N} \frac{e}{f_\Upsilon} \frac{2m_N}{(m_{P_b}^2 - m_N^2)m_\Upsilon} \times \sqrt{m_\Upsilon^2 (m_N^2 + 4m_N m_{P_b} + m_{P_b}^2) + (m_{P_b}^2 - m_N^2)^2}, \quad (9)$$

The Lagrangian depicting the coupling of the meson Υ with a photon reads as

$$\mathcal{L}_{\Upsilon\gamma} = -\frac{em_{\Upsilon}^2}{f_{\Upsilon}}V_{\mu}A^{\mu}, \quad (10)$$

where f_{Υ} is the Υ decay constant, respectively. Thus one gets the expression for the $\Upsilon \rightarrow e^+e^-$ decay,

$$\Gamma_{\Upsilon \rightarrow e^+e^-} = \left(\frac{e}{f_{\Upsilon}}\right)^2 \frac{8\alpha |\vec{p}_e^{\text{c.m.}}|^3}{3m_{\Upsilon}^2}, \quad (11)$$

where $\vec{p}_e^{\text{c.m.}}$ denotes the three-momentum of an electron in the rest frame of the Υ meson. The $\alpha = e^2/4\pi = 1/137$ is the electromagnetic fine structure constant. With the partial decay width of $\Upsilon \rightarrow e^+e^-$ [20], $\Gamma_{\Upsilon \rightarrow e^+e^-} \simeq 1.34$ keV, one gets $e/f_{\Upsilon} \simeq 0.0076$.

Since the partial decay widths $\Gamma_{P_b \rightarrow \Upsilon N}$ of the P_b states have been predicted in Ref. [35], the EM couplings related to the γNP_b vertices is also determined. In our previous work [23], the result shows that the experimental data point near the threshold is consistent with the contribution from the $P_c(4312)$ state by taking branching ratio $\text{Br}[P_c \rightarrow \pi N] \simeq 0.05\%$. In this paper, a small branching ratio of $\text{Br}[P_b \rightarrow \pi N] \simeq 0.05\%$ will also be used to calculate the coupling constant $g_{\pi NP_b}$. We will discuss this branching ratio in detail in the next section in conjunction with the values of cross section of P_b in the reaction $\pi^- p \rightarrow \Upsilon n$. The obtained coupling constants are listed in Table I by assuming that the πN channel accounts for 0.05% of total widths of P_b states.

TABLE I. The values of coupling constants by taking the decay width of $\Gamma_{P_b(11080) \rightarrow \Upsilon N} = 0.38$ MeV and $\Gamma_{P_b(11125) \rightarrow \Upsilon N} = 3.27$ MeV, while assuming the πN channel account for 0.05% of total widths of P_b states.

states	$\Gamma_{P_b \rightarrow \Upsilon N}$ (MeV)	$g_{P_b \Upsilon N}$	eh	$g_{P_b \pi N}$
$P_b(11080)$	0.38	0.074	0.00016	0.00049
$P_b(11125)$	3.27	0.213	0.00045	0.00145

B. Pomeron exchange and Reggeized t channel

For the P_b state photoproduction process, the Pomeron exchange is considered as the main background contribution. In this work, the dipole Pomeron model [42–44] is employed to calculate the cross section from the background contribution. The basic diagram is depicted in Fig. 1(c), where the Q^2 is the virtuality of the photon, and s and t are the Mandelstam variables. Generally, since the Regge model plays an important role in the high-energy process, a double Regge pole is also included in the dipole Pomeron model. Using the dipole Pomeron model and related parameters [43], the cross section of the reaction $\gamma p \rightarrow \Upsilon p$ can be calculated. Moreover, in Ref. [43], the result suggests that it may be more appropriate

when the value of the coefficient N_{Υ} is between N_{ϕ} and $N_{J/\psi}$. In our calculation, by taking $N_{\Upsilon} = \sqrt{2}/3$, the obtained cross section in dipole Pomeron model is well consistent with the experimental data [45–48], as shown in Fig. 3.

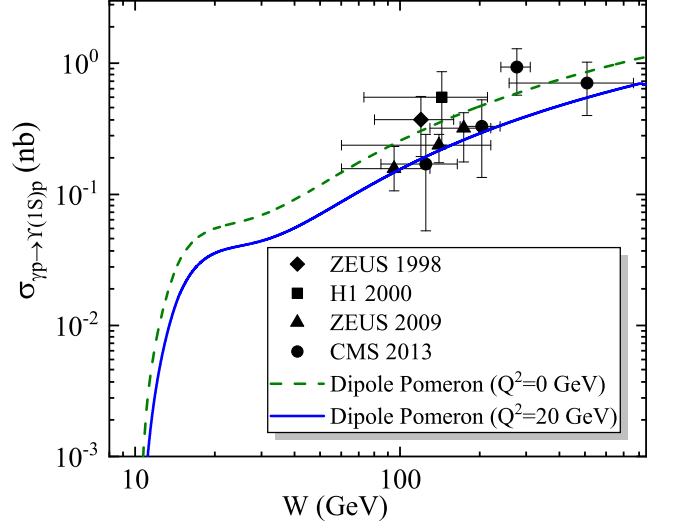


FIG. 3. Cross section for the reaction $\gamma p \rightarrow \Upsilon p$ with the dipole Pomeron model by taking the coefficient $N_{\Upsilon} = \sqrt{2}/3$. The green dashed, blue solid lines are for the Pomeron contributions with the $Q^2 = 0$ and 20 GeV, respectively. The experimental data are from Refs. [45–48].

For the P_b production via the reaction $\pi^- p \rightarrow \Upsilon n$, the background is mainly come from the t channel π , ρ , and ω exchanges, as depicted in Fig. 2(c). Since the branching ratios of Υ decaying into $\rho\pi$ and $\omega\pi$ channels are of the order of magnitude of 10^{-6} , the contributions from the ρ and ω exchanges should be very small and can be ignored. Therefore, in our calculation, only the contribution from the π exchange is considered. The effective Lagrangians for the vertices of $\Upsilon\pi\pi$ and πNN read as

$$\mathcal{L}_{\Upsilon\pi\pi} = -ig_{\Upsilon\pi\pi}(\pi^- \partial_{\mu}\pi^+ - \partial_{\mu}\pi^- \pi^+)\Upsilon^{\mu}, \quad (12)$$

$$\mathcal{L}_{\pi NN} = -ig_{\pi NN}\bar{N}\gamma_5\vec{\tau} \cdot \vec{\pi}N, \quad (13)$$

where N , π and Υ are the nucleon, the pion, and the Υ meson fields, respectively. Here, the $g_{\pi NN}^2/4\pi = 12.96$ is adopted [49]. Moreover, the coupling constant $g_{\Upsilon\pi\pi}$ can be determined from the decay width

$$\Gamma_{\Upsilon \rightarrow \pi\pi} = \frac{g_{\Upsilon\pi\pi}^2}{6\pi m_{\Upsilon}^2}|\vec{q}|^3,$$

where $|\vec{q}| = \sqrt{m_{\Upsilon}^2 - 4m_{\pi}^2}/2$. Taking the value of decay width $\Gamma_{\Upsilon \rightarrow \pi\pi}$ as 0.027 keV [20], one obtain the coupling constant $g_{\Upsilon\pi\pi} \simeq 0.0007$.

Since the energy corresponding to the $\pi^- p \rightarrow \Upsilon n$ reaction is above 10 GeV, the Reggeized treatment will be applied to the t channel process. Usually, one just need to replace the

Feynman propagator with the Regge propagator as

$$\frac{1}{t - m_\pi^2} \rightarrow \left(\frac{s}{s_{scale}}\right)^{\alpha_\pi(t)} \frac{\pi\alpha'_\pi}{\Gamma[1 + \alpha_\pi(t)] \sin[\pi\alpha_\pi(t)]}, \quad (14)$$

where the scale factor s_{scale} is fixed at 1 GeV. In addition, the Regge trajectories of $\alpha_\pi(t)$ is written as [23],

$$\alpha_\pi(t) = 0.7(t - m_\pi^2). \quad (15)$$

It can be seen that no free parameters have been added after the introduction of the Regge model.

C. Amplitude

Based on the Lagrangians above, the scattering amplitude for the reactions $\gamma p \rightarrow \Upsilon p$ and $\pi^- p \rightarrow \Upsilon n$ can be constructed as

$$-i\mathcal{M}_{\gamma p \rightarrow \Upsilon p} = \epsilon_\gamma^\nu(k_2) \bar{u}(p_2) \mathcal{A}_{\mu\nu} u(p_1) \epsilon_\gamma^\mu(k_1), \quad (16)$$

$$-i\mathcal{M}_{\pi^- p \rightarrow \Upsilon n} = \epsilon_\pi^\nu(k_2) \bar{u}(p_2) \mathcal{B}_{\mu\nu} u(p_1), \quad (17)$$

where u is the Dirac spinor of nucleon, and ϵ_Υ and ϵ_γ are the polarization vector of Υ meson and photon, respectively.

The reduced amplitude $\mathcal{A}_{\mu\nu}$ for the s channel P_b photoproduction reads

$$\mathcal{A}_{\mu\nu}^s = \frac{eh}{2m_N} g_{P_b \Upsilon N} \mathcal{F}_s(q_s^2) \gamma_5 \gamma_\nu \frac{(\not{q}_s + m_{P_b})}{q_s^2 - m_{P_b}^2 + im_{P_b} \Gamma_{P_b}} \gamma_\mu \not{k}_1, \quad (18)$$

and the reduced amplitude \mathcal{B}_μ for the s channel with P_b and t channel with π exchanges are written as

$$\mathcal{B}_\mu^s = \sqrt{2} g_{\pi N P_b} g_{P_b \Upsilon N} \mathcal{F}_s(q_s^2) \gamma_5 \gamma_\mu \frac{(\not{q}_s + m_{P_b})}{q_s^2 - m_{P_b}^2 + im_{P_b} \Gamma_{P_b}}, \quad (19)$$

$$\mathcal{B}_\mu^t = \sqrt{2} g_{\Upsilon \pi \pi} g_{\pi N N} \frac{\mathcal{F}_t(q_t^2)}{q_t^2 - m_\pi^2} \gamma_5 k_{1\mu}, \quad (20)$$

where $q_s = k_1 + p_1$ and $q_t = k_1 - k_2$ are the four-momenta of the exchanged P_b state in s channel and π meson in t channel, respectively.

For the s channel with intermediate P_b state, one adopts a general form factor to describe the size of hadrons as [22, 23, 38],

$$\mathcal{F}_s(q_s^2) = \frac{\Lambda^4}{\Lambda^4 + (q_s^2 - m_{P_b}^2)^2}, \quad (21)$$

where q_s and m_{P_b} are the four-momentum and mass of the exchanged P_b state, respectively. For the heavier hadron production, the typical value of cutoff $\Lambda = 0.5$ GeV will be taken as used in Refs. [22, 23, 38].

For the t -channel meson exchanges [23, 38], the general form factor $\mathcal{F}_t(q_t^2)$ consisting of $\mathcal{F}_{\Upsilon\pi\pi} = (\Lambda_t^2 - m_\pi^2)/(\Lambda_t^2 - q_t^2)$ and $\mathcal{F}_{\pi NN} = (\Lambda_t^2 - m_\pi^2)/(\Lambda_t^2 - q_t^2)$ are taken into account. Here, q_π and m_π are 4-momentum and mass of the π meson, respectively. The value of the cutoff Λ_t is taken as 2.0 GeV, which is the same as that in Ref. [23].

III. NUMERICAL RESULTS

With the preparation in the previous section, the cross section of the reaction $\gamma p \rightarrow \Upsilon p$ can be calculated. The differential cross section in the center of mass (c.m.) frame is written as

$$\frac{d\sigma}{d\cos\theta} = \frac{1}{32\pi s} \frac{|\vec{k}_2^{\text{c.m.}}|}{|\vec{k}_1^{\text{c.m.}}|} \left(\frac{1}{J} \sum_\lambda |\mathcal{M}|^2 \right), \quad (22)$$

with $J = 4$ for the $\gamma p \rightarrow \Upsilon p$ reaction and $J = 2$ for the reaction $\pi^- p \rightarrow \Upsilon n$. Here, $s = (k_1 + p_1)^2$, and θ denotes the angle of the outgoing Υ meson relative to π/γ beam direction in the c.m. frame. $\vec{k}_1^{\text{c.m.}}$ and $\vec{k}_2^{\text{c.m.}}$ are the three-momenta of the initial photon beam and final Υ meson, respectively.

A. P_b production in reaction $\gamma p \rightarrow \Upsilon p$

In Fig. 4 we present the total cross section for the reaction $\gamma p \rightarrow \Upsilon p$ from threshold to 800 GeV of the center of mass energy. It is found that the contribution from pentaquark P_b state shows a very sharp peak near the threshold, and the experimental point at high energy is well consistent with the cross section of the Pomeron diffractive process.

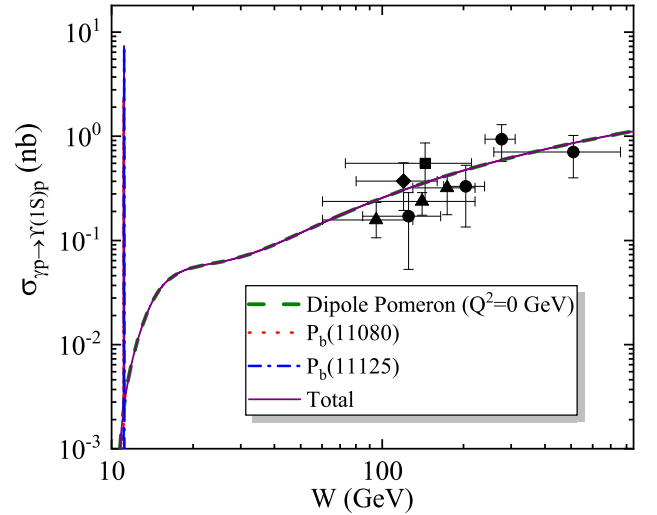


FIG. 4. Total cross section for the reaction $\gamma p \rightarrow \Upsilon p$. The green dashed, red dotted, blue dot-dashed, and violet solid lines are for the Pomeron, the $P_b(11080)$, the $P_b(11125)$, and total contributions, respectively. The experimental data are taken from Refs. [45–48].

In order to more clearly distinguish the contributions from the P_b states, in Fig. 5 we give the same results as Fig. 4 but with a reduced energy range. As can be seen from Fig. 5, when the energy bin width is chosen as 0.01 GeV, two distinct peaks can be seen around 11 GeV, which are derived from the contributions of states $P_b(11080)$ and $P_b(11125)$, respectively. Since the mass of $P_b(11080)$ and $P_b(11125)$ are very close to each other, if we increase the bin width to 0.1 GeV, it is

difficult to distinguish the two peaks, and a larger bump will be formed, as shown in Fig. 6. Therefore, if different P_b signals need to be distinguished, a small energy bin width is needed.

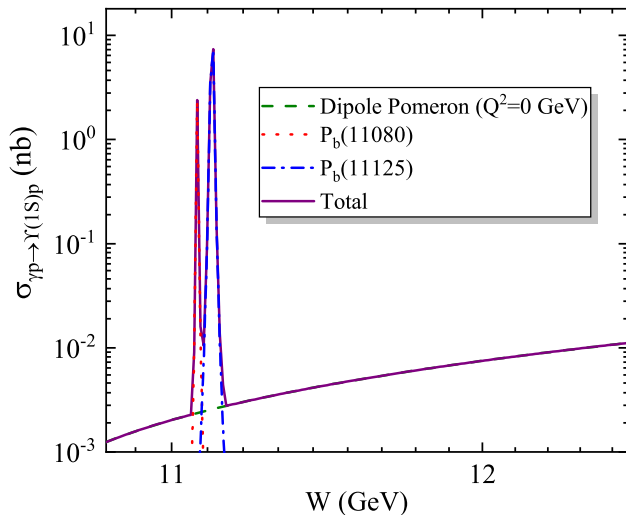


FIG. 5. Same as Fig. 4 except that the energy range is reduced.

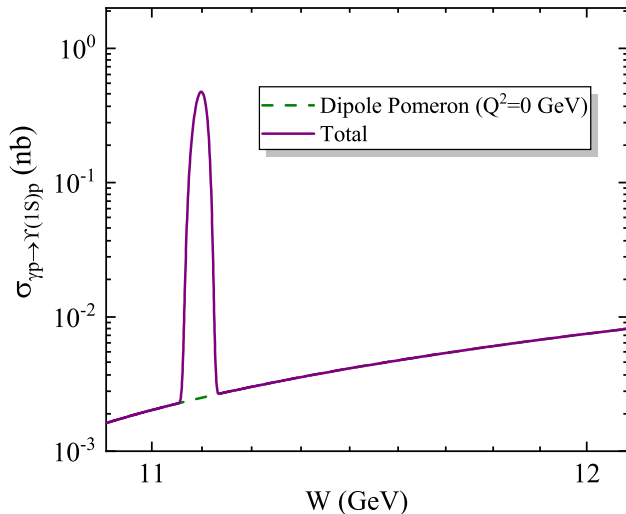


FIG. 6. Same as Fig. 5 except that the energy bin width is increased to 0.1 GeV.

Moreover, the result suggests that the theoretical average of the cross section from the $P_b(11080)$ is of a order of magnitude of 1 nb if the bin width is 0.01 GeV. If the bin width increases to 0.1 GeV, the theoretical average value of the cross section of $P_b(11080)$ becomes about 0.3 nb. In Refs. [50, 51], the cross section of process $\gamma p \rightarrow \Upsilon p$ at 11 GeV was estimated to be about 12 pb – 50 pb. Even if the background cross section can reach this magnitude, as long as the bin width is less than or equal to 0.1 GeV, the possibility of distinguishing the P_b state from the background is great.

B. P_b production in reaction $\pi^- p \rightarrow \Upsilon n$

In Fig. 7, the total cross section of the interaction $\pi^- p \rightarrow \Upsilon n$ is presented. It can be seen that near the threshold, the background cross section from the t channel is very small, even if we take a value of cutoff as 2.0 GeV. The main reason for this situation is that the branching ratio of Υ decaying into $\pi\pi$ channel is very small, and the branching ratios of Υ decaying to $\rho\pi$ and $\omega\pi$ channels are smaller and can be ignored. Near the threshold, we can see very sharp peaks, which come from the contribution of the P_b states.

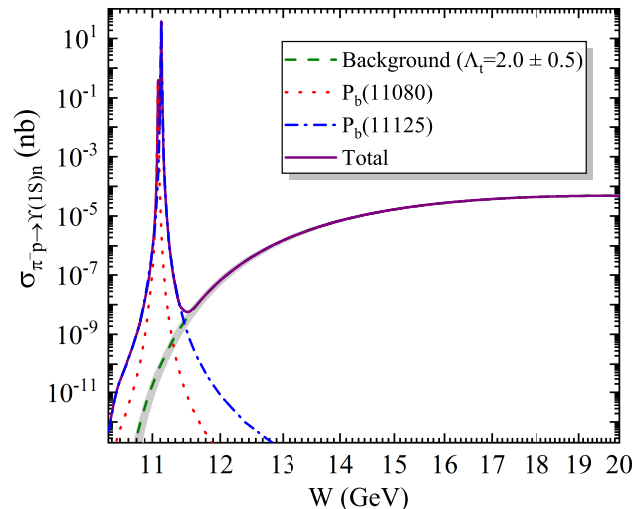


FIG. 7. Total cross section for the reaction $\pi^- p \rightarrow \Upsilon n$. The green dashed, red dotted, blue dot-dashed, and violet solid lines are for the background, the $P_b(11080)$, the $P_b(11125)$, and total contributions, respectively. The bands stand for the error bar of the cutoff Λ_t .

To more clearly distinguish the cross section at the threshold, we present more explicit near the threshold in Fig. 8, which is the same as the Fig. 7 except that the energy range is reduced. One find that the total cross section exhibits two peaks around the 11 GeV when the bin width is taken to be 0.01 GeV. According to our calculation, when the bin width is 0.1 GeV, branching ratio of $\text{Br}[P_b \rightarrow \pi N] \simeq 0.05\%$, the theoretical average value of the cross section from the $P_b(11080)$ state reaches at least 0.1 nb in a bin interval, which is several orders of magnitude higher than the background cross section.

Specifically, when we take the branching ratio of P_b to πN as 0.0005%, the corresponding coupling constants $g_{P_b(11080)\pi N}$ and $g_{P_b(11125)\pi N}$ are 0.000049 and 0.000145, respectively. According to the obtained coupling constants, the total cross section of the reaction $\pi^- p \rightarrow \Upsilon n$ is given when the energy bin width is 0.01 GeV, as shown in Fig. 9. One notice that the signal is still much higher than the background. Even increasing the energy bin width to 0.1 GeV, the theoretical average of the cross section from the $P_b(11080)$ can reach the order of 0.001 nb, which means that the signal is still clearly distinguished from the background.

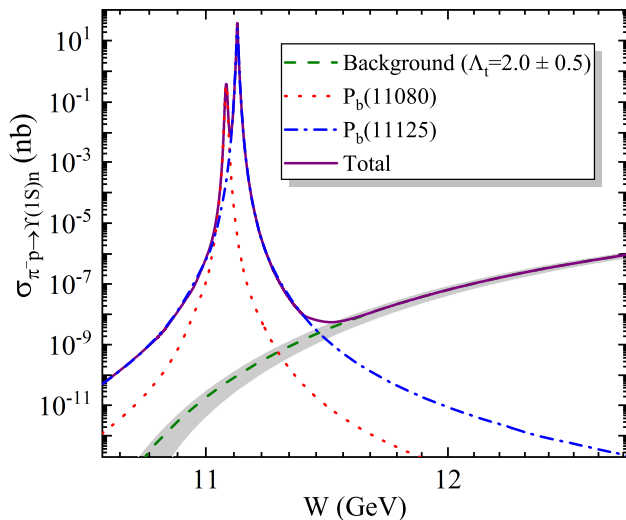


FIG. 8. Same as Fig. 7 except that the energy range is reduced.

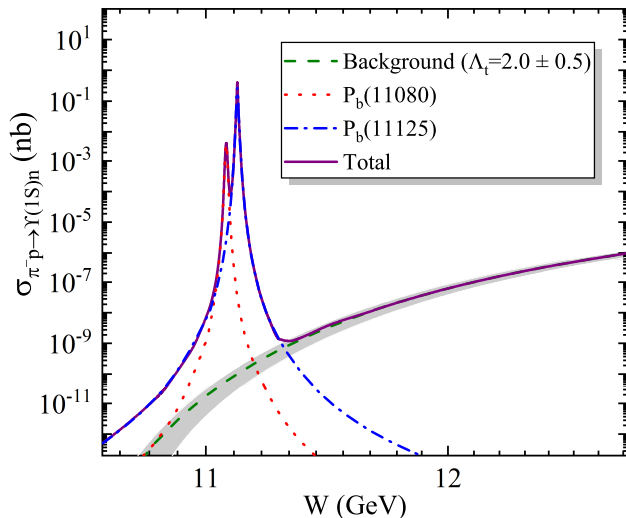


FIG. 9. Same as Fig. 8 except that the branching ratio of P_b to πN is reduced to 0.0005%.

IV. SUMMARY AND DISCUSSION

The pentaquark is an important kind of the exotic hadron. The observation of the P_c states at LHCb inspires us to predict the possible hidden-bottom pentaquark. Since it is impossible to decay from a heavy hadrons as P_c states, it is interesting to study production of hidden-bottom pentaquarks through exciting nucleon by photon or pion. In this work, based on the effective field theory and the VMD mechanism, the production of the hidden-bottom pentaquark P_b states via γp or $\pi^- p$ scattering is investigated.

For the background of the P_b state photoproduction, it is thought that it mainly comes from the contribution of the Pomeron exchange. Using the dipole pomeron model, the

experimental data of the interaction $\gamma p \rightarrow \Upsilon p$ can be well described. Near the threshold, when the bin width is 0.01 GeV, very sharp peaks from the P_b states can be clearly distinguished in the cross sections. According to our calculation, even if the bin width is increased to 0.1 GeV, the cross section of the P_b signal is still higher than the background, which means that the vicinity of the center of mass energy of 11 GeV is the best energy window for searching for these P_b states via the photoproduction process. It is suggested that experiments to search for the P_b states through the γp scattering can be carried out, which is well within the capabilities of the COMPASS facility at CERN [52].

For the production of the P_b states in the reaction $\pi^- p \rightarrow \Upsilon n$, the background is considered to be mainly derived from the contribution of the Reggeized t channel with π exchange. Since the branching ratio of the P_b decaying into $\pi\pi$ channel is very small, the background cross section of the process $\pi^- p \rightarrow \Upsilon n$ is several orders of magnitude lower than the cross section from the P_b signal. According to our calculation, even if the branching ratio of the P_b into πN channel is reduced to 0.0005%, the average value of the cross section from $P_b(11080)$ contribution reaches an order of 0.001 nb/100 MeV, which is still much higher than the background contribution. Compared to the photoproduction process, the requirement of experimental precision for searching for these P_b states by the $\pi^- p$ scattering may be lower, which indicates that searching for the process P_b via $\pi^- p \rightarrow \Upsilon n$ may be a very important and promising way. Hence, an experimental study of the hidden bottom pentaquark P_b states via the pion-induced reaction is strongly suggested, which can be carried on the J-PARC and COMPASS facilities [52, 53].

In addition, since both the electromagnetic γp and ep reactions are very similar, we also look forward to finding and studying these hidden bottom pentaquark P_b states through the ep scattering process. Electromagnetic probes covering the above energy are expected to be produced on future EicC (Electron Ion Collider in China) facility in China. The accumulated luminosity with one-year run is about 50fb^{-1} [54, 55]. Because such facility is usually impossible to run near a fixed energy point for a year, we make an estimation of one-day run, that is, an accumulated luminosity about 0.1fb^{-1} . The number of events reaches $1 \times 10^5/0.01\text{ GeV}$ near the mass of the P_b state if we adopt a cross section $1\text{nb}/0.01\text{ GeV}$ predicted in our calculation. Even after considering the efficiency and the uncertainty of theoretical prediction, which may depress the number of event by two or three orders of magnitude, the observation of hidden-bottom pentaquarks is still very promising at EicC.

V. ACKNOWLEDGMENTS

This project is supported by the National Natural Science Foundation of China under Grants No. 11705076 and No. 11675228. We acknowledge the supported by the Key Research Program of the Chinese Academy of Sciences, Grant NO. XDPB09. This work is partly supported by HongLiu Support Funds for Excellent Youth Talents of Lanzhou University of Technology.

- [1] R. Aaij *et al.* [LHCb Collaboration], “Observation of a narrow pentaquark state, $P_c(4312)^+$, and of two-peak structure of the $P_c(4450)^+$,” *Phys. Rev. Lett.* **122**, no. 22, 222001 (2019)
- [2] R. Aaij *et al.* [LHCb Collaboration], “Observation of $J/\psi p$ Resonances Consistent with Pentaquark States in $\Lambda_b^0 \rightarrow J/\psi K^- p$ Decays,” *Phys. Rev. Lett.* **115**, 072001 (2015)
- [3] M. Z. Liu, Y. W. Pan, F. Z. Peng, M. Snchez Snchez, L. S. Geng, A. Hosaka and M. Pavon Valderrama, “Emergence of a complete heavy-quark spin symmetry multiplet: seven molecular pentaquarks in light of the latest LHCb analysis,” *Phys. Rev. Lett.* **122**, no. 24, 242001 (2019)
- [4] J. He, “Study of $P_c(4457)$, $P_c(4440)$, and $P_c(4312)$ in a quasipotential Bethe-Salpeter equation approach,” *Eur. Phys. J. C* **79**, 393 (2019).
- [5] R. Chen, Z. F. Sun, X. Liu and S. L. Zhu, “Strong LHCb evidence supporting the existence of the hidden-charm molecular pentaquarks,” *Phys. Rev. D* **100**, no. 1, 011502 (2019)
- [6] H. X. Chen, W. Chen and S. L. Zhu, “Possible interpretations of the $P_c(4312)$, $P_c(4440)$, and $P_c(4457)$,” *Phys. Rev. D* **100**, no. 5, 051501 (2019)
- [7] H. Huang, J. He and J. Ping, “Looking for the hidden-charm pentaquark resonances in $J/\psi p$ scattering,” arXiv:1904.00221 [hep-ph].
- [8] A. Ali and A. Y. Parkhomenko, “Interpretation of the narrow $J/\psi p$ Peaks in $\Lambda_b \rightarrow J/\psi p K^-$ decay in the compact diquark model,” *Phys. Lett. B* **793**, 365 (2019)
- [9] C. J. Xiao, Y. Huang, Y. B. Dong, L. S. Geng and D. Y. Chen, “Exploring the molecular scenario of $P_c(4312)$, $P_c(4440)$, and $P_c(4457)$,” *Phys. Rev. D* **100**, no. 1, 014022 (2019)
- [10] Z. H. Guo and J. A. Oller, “Anatomy of the newly observed hidden-charm pentaquark states: $P_c(4312)$, $P_c(4440)$ and $P_c(4457)$,” *Phys. Lett. B* **793**, 144 (2019).
- [11] C. W. Xiao, J. Nieves and E. Oset, “Heavy quark spin symmetric molecular states from $\bar{D}^{(*)}\Sigma_c^{(*)}$ and other coupled channels in the light of the recent LHCb pentaquarks,” *Phys. Rev. D* **100**, no. 1, 014021 (2019)
- [12] F. K. Guo, H. J. Jing, U. G. Meiner and S. Sakai, “Isospin breaking decays as a diagnosis of the hadronic molecular structure of the $P_c(4457)$,” *Phys. Rev. D* **99**, no. 9, 091501 (2019)
- [13] C. Fernandez-Ramirez *et al.* [JPAC Collaboration], “Interpretation of the LHCb $P_c(4312)^+$ Signal,” *Phys. Rev. Lett.* **123**, no. 9, 092001 (2019).
- [14] R. Zhu, X. Liu, H. Huang and C. F. Qiao, “Analyzing doubly heavy tetra- and penta-quark states by variational method,” *Phys. Lett. B* **797**, 134869 (2019).
- [15] Q. Wu and D. Y. Chen, “Production of P_c states from Λ_b decay,” *Phys. Rev. D* **100**, no. 11, 114002 (2019).
- [16] M. B. Voloshin, “Some decay properties of hidden-charm pentaquarks as baryon-meson molecules,” *Phys. Rev. D* **100**, no. 3, 034020 (2019).
- [17] Y. H. Lin and B. S. Zou, “Strong decays of the latest LHCb pentaquark candidates in hadronic molecule pictures,” *Phys. Rev. D* **100**, no. 5, 056005 (2019).
- [18] J. He and D. Y. Chen, “Molecular states from $\Sigma_c^{(*)}\bar{D}^{(*)} - \Lambda_c\bar{D}^{(*)}$ interaction,” *Eur. Phys. J. C* **79**, no. 11, 887 (2019).
- [19] S. G. Yuan, K. W. Wei, J. He, H. S. Xu and B. S. Zou, “Study of $qqqc\bar{c}$ five quark system with three kinds of quark-quark hyperfine interaction,” *Eur. Phys. J. A* **48**, 61 (2012)
- [20] M. Tanabashi *et al.* [ParticleDataGroup], “Review of Particle Physics,” *Phys. Rev. D* **98**, 030001 (2018).
- [21] Y. Huang, J. He, H. F. Zhang and X. R. Chen, “Discovery potential of hidden charm baryon resonances via photoproduction,” *J. Phys. G* **41**, no. 11, 115004 (2014)
- [22] X. Y. Wang, X. R. Chen and J. He, “Possibility to study pentaquark states $P_c(4312)$, $P_c(4440)$, and $P_c(4457)$ in $\gamma p \rightarrow J/\psi p$ reaction,” *Phys. Rev. D* **99**, 114007 (2019).
- [23] X. Y. Wang, J. He, X. R. Chen, Q. Wang and X. Zhu, “Pion-induced production of hidden-charm pentaquarks $P_c(4312)$, $P_c(4440)$, and $P_c(4457)$,” *Phys. Lett. B* **797**, 134862 (2019).
- [24] A. Ali *et al.* [GlueX Collaboration], “First Measurement of Near-Threshold J/ψ Exclusive Photoproduction off the Proton,” *Phys. Rev. Lett.* **123**, 072001 (2019).
- [25] J. He, *Phys. Lett. B* **753**, 547 (2016) doi:10.1016/j.physletb.2015.12.071 [arXiv:1507.05200 [hep-ph]].
- [26] Z. C. Yang, Z. F. Sun, J. He, X. Liu and S. L. Zhu, “The possible hidden-charm molecular baryons composed of anti-charmed meson and charmed baryon,” *Chin. Phys. C* **36**, 6 (2012)
- [27] J. J. Wu and B. S. Zou, “Prediction of super-heavy N^* and Λ^* resonances with hidden beauty,” *Phys. Lett. B* **709**, 70 (2012).
- [28] C. W. Xiao and E. Oset, “Hidden beauty baryon states in the local hidden gauge approach with heavy quark spin symmetry,” *Eur. Phys. J. A* **49**, 139 (2013).
- [29] J. Wu, Y. R. Liu, K. Chen, X. Liu and S. L. Zhu, “Hidden-charm pentaquarks and their hidden-bottom and B_c -like partner states,” *Phys. Rev. D* **95**, no. 3, 034002 (2017).
- [30] Y. Yamaguchi, A. Giachino, A. Hosaka, E. Santopinto, S. Takeuchi and M. Takizawa, “Hidden-charm and bottom meson-baryon molecules coupled with five-quark states,” *Phys. Rev. D* **96**, no. 11, 114031 (2017).
- [31] J. Ferretti, E. Santopinto, M. Naeem Anwar and M. A. Bedolla, “The baryo-quarconium picture for hidden-charm and bottom pentaquarks and LHCb $P_c(4380)$ and $P_c(4450)$ states,” *Phys. Lett. B* **789**, 562 (2019).
- [32] G. Yang, J. Ping and J. Segovia, “Hidden-bottom pentaquarks,” *Phys. Rev. D* **99**, no. 1, 014035 (2019).
- [33] H. Huang and J. Ping, “Investigating the hidden-charm and hidden-bottom pentaquark resonances in scattering process,” *Phys. Rev. D* **99**, no. 1, 014010 (2019)
- [34] B. Wang, L. Meng and S. L. Zhu, “Hidden-charm and hidden-bottom molecular pentaquarks in chiral perturbation theory,” *JHEP* **1911**, 108 (2019).
- [35] T. Gutsche and V. E. Lyubovitskij, “Structure and decays of hidden heavy pentaquarks,” *Phys. Rev. D* **100**, no. 9, 094031 (2019).
- [36] X. Y. Wang and J. He, “ $K^{*0}\Lambda$ photoproduction off a neutron,” *Phys. Rev. C* **93**, 035202 (2016).
- [37] X. Y. Wang, J. He and H. Haberzettl, “Analysis of recent CLAS data on $\Sigma^*(1385)$ photoproduction off a neutron target,” *Phys. Rev. C* **93**, 045204 (2016).
- [38] S. H. Kim, S. i. Nam, Y. Oh and H. C. Kim, “Contribution of higher nucleon resonances to $K^*\Lambda$ photoproduction,” *Phys. Rev. D* **84**, 114023 (2011).
- [39] T. H. Bauer, R. D. Spital, D. R. Yennie and F. M. Pipkin, “The Hadronic Properties of the Photon in High-Energy Interactions,” *Rev. Mod. Phys.* **50**, 261 (1978) Erratum: [*Rev. Mod. Phys.* **51**, 407 (1979)]. doi:10.1103/RevModPhys.50.261
- [40] T. Bauer and D. R. Yennie, “Corrections to VDM in the Photoproduction of Vector Mesons. I. Mass Dependence of Amplitudes,” *Phys. Lett.* **60B**, 165 (1976).

- [41] T. Bauer and D. R. Yennie, “Corrections to Diagonal VDM in the Photoproduction of Vector Mesons. 2. Phi-omega Mixing,” *Phys. Lett.* **60B**, 169 (1976).
- [42] E. Martynov, E. Predazzi and A. Prokudin, “A Universal Regge pole model for all vector meson exclusive photoproduction by real and virtual photons,” *Eur. Phys. J. C* **26**, 271 (2002).
- [43] E. Martynov, E. Predazzi and A. Prokudin, “Photoproduction of vector mesons in the soft dipole pomeron model,” *Phys. Rev. D* **67**, 074023 (2003).
- [44] X. Cao, F. K. Guo, Y. T. Liang, J. J. Wu, J. J. Xie, Y. P. Xie, Z. Yang and B. S. Zou, “Photoproduction of hidden-bottom pentaquark and related topics,” arXiv:1912.12054 [hep-ph].
- [45] J. Breitweg *et al.* [ZEUS Collaboration], “Measurement of elastic Upsilon photoproduction at HERA,” *Phys. Lett. B* **437**, 432 (1998).
- [46] S. Chekanov *et al.* [ZEUS Collaboration], “Exclusive photoproduction of upsilon mesons at HERA,” *Phys. Lett. B* **680**, 4 (2009).
- [47] C. Adloff *et al.* [H1 Collaboration], “Elastic photoproduction of J/ψ and Upsilon mesons at HERA,” *Phys. Lett. B* **483**, 23 (2000).
- [48] CMS Collaboration [CMS Collaboration], “Measurement of exclusive Y photoproduction in pPb collisions at $\sqrt{s_{NN}} = 5.02$ TeV,” CMS-PAS-FSQ-13-009.
- [49] Z. W. Lin, C. M. Ko and B. Zhang, “Hadronic scattering of charm mesons,” *Phys. Rev. C* **61**, 024904 (2000).
- [50] M. Karliner and J. L. Rosner, “Photoproduction of Exotic Baryon Resonances,” *Phys. Lett. B* **752**, 329 (2016).
- [51] S. Aid *et al.* [H1 Collaboration], “Elastic and inelastic photoproduction of J/ψ mesons at HERA,” *Nucl. Phys. B* **472**, 3 (1996).
- [52] F. Nerling [COMPASS Collaboration], “Hadron Spectroscopy with COMPASS: Newest Results,” *EPJ Web Conf.* **37**, 01016 (2012).
- [53] S. Kumano, “Spin Physics at J-PARC,” *Int. J. Mod. Phys. Conf. Ser.* **40**, 1660009 (2016).
- [54] X. Chen, “A Plan for Electron Ion Collider in China,” *PoS DIS* **2018**, 170 (2018).
- [55] X. Chen, “Electron - Ion Collider in China,” *PoS SPIN* **2018**, 160 (2019).